FACTORIAL EXPERIMENTAL DESIGN FOR DETERMINING BIOMASS THERMOCHEMICAL TREATMENT AND PURE HYDROCARBONS ADSORPTION PARAMETERS

Dimitrios K. Sidiras*, Fragiskos A. Batzias, Christina G. Siontorou, Athanasia N. Bountri, Dorothea V. Politi, Odysseas N. Kopsidas, Ilias G. Konstantinou, George N. Katsamas, Ioanna S. Salapa, Stavroula P. Zervopoulou
Lab. Simulation of Industrial Processes, Dep. Industrial Management and Technology, Univ. Piraeus
80 Karaoli & Dimitriou, GR 18534 Piraeus, Greece

ABSTRACT: The thermochemical treatment of lignocellulosic waste biomass can provide low-cost adsorbents with increased sorption capacity and biodegradability for cleaning by adsorption the hydrocarbon spills. This work deals with the planning and carrying out the experimental measurements necessary to cover some combinations of lignocellulosic adsorbent materials and hydrocarbons to be adsorbed. The kinds of lignocellulosic waste adsorbents examined herein were selected by means of multicriteria analysis and subsequently studied with a view to correlating their physicochemical properties with surface topography and chemical composition. The SEM surface topography, the BET surface area and the XRD patterns for untreated and modified wheat straw were also studied. Optimal modification conditions, for maximizing the diesel and crude oil adsorptivity, were found by means of factorial experimental design. Diesel and crude oil spills were formed on seawater (two Ports), stream water and lake water. The diesel and crude oil adsorption on untreated and pretreated wheat straw was measured. The diesel and crude oil adsorption on pretreated wheat straw was significantly higher compared to that of the untreated material.
Keywords: adsorbent, hydrolysis, chemical composition, cellulose, lignin, biomass.

1 INTRODUCTION

Aromatic hydrocarbons, alkanes, alkenes, cycloalkanes and alkyne-based compounds are different types of hydrocarbons. The majority of hydrocarbons occur in crude oil, where decomposed organic matter provides an abundance of carbon and hydrogen which can be bonded in various ways. Oil is one of the major resources of energy in the present industrialized world. Given that oil is explored, transported, stored, and used, there will always be the threat of oil pollution. Oil spills in marine aquatic environment may be due to releases of oil from offshore platforms, drilling rigs, underwater pipeline raptures, routine oil tanker operations or nautical accidents such as collisions, groundings, hull failures, fires and explosions. Occasionally, sea waters can be oil polluted by natural seepage mainly in the ocean. Oil spills cause great damage to the coastal environment, mainly in sensitive marine ecosystems, and negative economical impacts on tourism and fisheries. Chemical dispersion, in situ burning, mechanical containment and oil sorption by adsorbents are the generally cleanup methods to combat the oil pollution. Adsorbents concentrate and transform liquid oil to the semi solid or solid phase, which can be removed from seawater. These materials can be divided into three basic categories: (i) inorganic mineral, (ii) organic synthetic and (iii) natural organic products like waste lignocellulosic biomass or agro-industrial by-products [1]. The modification of such wastes can provide adsorbents with relatively high sorption capacity, biodegradability, and cost-effectiveness for the adsorption of dyes, heavy metals and oil products [2-9].

Straws are renewable materials for production of cellulose, glucose, bioethanol and other chemicals. Straws are often used during containment and cleanup of oil spills. In this case, the surface properties of straws play a crucial role. When straws are employed for restrictions of algae growth, suitable surface properties allow microorganisms and fungi to adhere and decompose the straw. As a result, substances responsible for decreasing lake blooms are released. Since leaves and stems are the main components of straw, the surfaces of these plant parts must be considered in order to understand these phenomena. The thin wax layer covering stalks and leaves of cereals is composed of esters, long chain fatty acids and monohydroxy alcohols, therefore straw should favourably adsorb hydrophobic liquids. Waxes are insoluble in water, thus the coating on external surfaces of stems, leaves, flowers, fruits and seeds protects them from excessive water evaporation or outer moisture. Waxes also protect plants from microorganisms and mechanical damage. Wax coating aids the process of crop ripening by preventing stalks from becoming moist again. Straw like the other adsorbing material is capable of holding oil as the result of two processes: adsorption and absorption. Wax coverage making the straw surface hydrophobic (as well as capillary forces) determines the efficiency of oil removal. The adsorption capacity depends primarily on the chemical structure of straw tissue that has direct contact with oil. The absorption capacity is a function of the structure of the straw stalks in the bundles, distances between them, the diameter and cross-sections of each stalk and leaf. Due to high oil adsorption by straw, oil is mostly held due to capillary of straw tissue and interior part of stalk, as well as to the existence of oil bridges between stalks. Straw adsorption capacity varies according to many researches, due to different apparent densities of straw and its structure. The absorption of oil depends on both, the surface properties and the interior structure of straw [10].

A survey of literature shows that walnut shell [1], biomass [11], raw bagasse [12], carbonized pith bagasse [13], acetylated sugarcane bagasse [14], peat [15-16], fatty acid grafted straw [17], carbonized fir fibers [18], barley straw [10, 19-22], wheat straw [23], rice straw [24], rice husk [25-26], sludge, garlic and onions peels [27], banana trunk fiber [28], and groundnut husks [29], can be used as adsorbents for oil-spills.

This work deals with the planning, and carrying out in a systematic way, the experimental measurements necessary to cover some combinations adsorbent materials and hydrocarbons to be used as adsorbates. The hydrocarbon mixtures were either supplied by Hellenic Petroleum SA or prepared by fractional distillation using the physical simulator at the Laboratory of Simulations of Industrial Processes of the University of Piraeus. The

Table I: Composition of wheat straw.

Component	% w/w
Cellulose	32.7
Hemicelluloses	24.5
• Xylose	19.3
• Arabinose	2.7
• Acetyl groups	2.5
Klason lignin (acid insoluble)	16.8
Ash	4.7
Extractives	6.2
Other components	15.1

kinds of lignocellulosic waste adsorbents, suggested by the multicriteria analysis [30], were studied with a view to correlating their physicochemical properties with surface topography and chemical composition [31, 32]. The SEM surface topography, the BET surface area, and the XRD patterns for untreated and modified wheat straw were also studied. Diesel and crude oil spills were formed on seawater (two Ports), stream water and lake water to provide adsorbate on real basis. The diesel adsorption on untreated and pretreated wheat straw was measured and compared to the corresponding results obtained when commercial adsorbents are used.

2 MATERIALS AND METHODS

2.1 Material origin

The wheat straw used in this work was obtained from the Kapareli village, close to the Thiva city at the Kopaida area in central Greece (harvesting year 2012), as a suitable source for full-scale industrial applications. The moisture content of the material when received was 8.8% w/w; after screening, the fraction with particle sizes between 10 and 20 mm was isolated. The composition is presented in Table I.

Commercial polypropylene oil adsorbent pad 'Scorpion P-200' and pom poms oil trap (both manufactured by New Naval Ltd. located in Piraeus, Greece) were used to compare their adsorbency to the untreated and modified wheat straw.

2.2. The autohydrolysis modification process

The wheat straw autohydrolysis process was performed in a 3.75-L batch reactor PARR 4843. The autohydrolysis isothermal time was 0-50 min (not including the preheating time); the reaction was catalyzed by the organic acids produced by the wheat straw itself during autohydrolysis at a liquid-to-solid ratio of 20:1; the liquid phase volume (water) was 2000 mL and the solid material dose (wheat straw or barley straw) was 100 g. The reaction ending temperature was 160°C, 180°C, 200°C and 240°C, reached after the 44, 47, 66 and 80 min preheating time, respectively.

2.3 The maleic acid hydrolysis modification process

The wheat straw was pretreated by hydrolysis catalyzed with maleic acid ($C_4H_4O_4$) [33]; the acid hydrolysis process was performed in a 3.75-L batch reactor PARR 4843. The acid hydrolysis time was 0-50

min (isothermal acid hydrolysis time-periods not including the preheating time; preheating time must be added to these isothermal time-periods to give the 'Total Acid Hydrolysis Time'); the reaction was catalyzed by maleic acid 0.01-0.09 M during acid hydrolysis process at a liquid-to-solid ratio of 20:1; the liquid phase volume was 2000 mL the solid material dose (wheat straw) was 100 g. The reaction ending temperature was 140 °C – 180 °C, reached after the 35 - 50 min preheating time-periods, respectively.

2.4. Adsorption isotherm studies

Methylene Blue (MB) adsorption isotherms were derived from batch experiments. Following the batch procedure, accurately weighed quantities of adsorbent were transferred into 0.8-L bottles, where 0.5 L of adsorbate solution was added. The sorbent weight varied from 0.5 g to 3 g, the temperature was 23 °C, the initial Methylene Blue (MERCK, C.I. 52015) concentration varied from 1.4 mg/L to 156 mg/L. The bottles were sealed and mechanically tumbled for a period of 7 days. This time period was chosen after experimental studies (the initial time interval was from 4 h to 14 days), to ensure that nearly equilibrium conditions were achieved. The resulting solution concentrations were determined and the equilibrium data from each bottle represented one point on the adsorption isotherm plots.

2.5. Kinetic studies

Methylene Blue adsorption rate batch experiments were conducted in a 2-L completely mixed glass reactor fitted with a twisted blade-type stirrer, operating at 300 rpm for keeping the lignocellulosic material in suspension. The reactor, containing 1 L aqueous dye solution, was placed into a water bath to keep temperature constant at the desired level. The sorbent weight varied from 1 g to 6 g, the temperature varied from 10 to 55 °C, the initial Methylene Blue concentration varied from 1.4 mg/L to 156 mg/L. The effect of stirring was studied in the rage of 0 to 600 rpm. The pH effect was studied in the range of 1.5 to 13 (the initial pH of the dye solutions was adjusted using dilute H_2SO_4 or NaOH solutions, as appropriate).

2.6 Analytical Techniques

The study of untreated and pretreated wheat and barley straw samples by scanning electron microscopy, SEM, was conducted at the Institute of Materials Science of the National Center for Scientific Research 'Demokritos' using an FEI INSPECT SEM equipped with an EDAX super ultra thin window analyzer for energy dispersive X-ray spectroscopy (EDS). The magnification was X75, X750, X7,500 and X20,000.

The BET (Brunauer, Emmet and Teller) surface area of the untreated and the pretreated pine sawdust was measured from the N_2 adsorption isotherm with a Nova® Surface Area Analyzer (Quantachrome Instruments) in accordance with DIN 66132 [34]. Prior to this measurement, the samples were dried under vacuum at 150 °C overnight to clean the surface. The experimental data were analyzed using the "Quantachrome NovaWin2 Data Acquisition and Reduction for NOVA instruments" software.

The powder XRD patterns of the origin and the pretreated samples were measured on by a SIEMENS

Table II. Quality specifications of diesel 10 PPM and crude oil.

Properties	Units	Results
Diesel oil quality specifications		
Density at 15°C	kg/m³	823.0
Color		L0.5
%(v/v) Rec. at 250 °C	%v/v	35.3
%(v/v) Rec. at 350 °C	%v/v	94.6
95%(v/v) Recovered	°C	359.0
Flash point	°C	61.5
Sulfur content	mg/kg	2.2
Copper strip corrosion (3 h at 50 °C)	Class	1a
CFPP	°C	-17
Viscosity at 40 °C	cST	2.772
Water content	mg/kg	45
Cetane number		54.0
Cetane index		57.9
Ash content	% m/m	0.003
Carbon residue (on 10% distill. residue)	%m/m	0.01
Total contamination	mg/kg	5.0
Oxidation stability	g/m³	3.4
Polycyclic aromatic hydrocarbons	%m/m	0.6
Lubricity, corrected (wsd1.4) at 60 °C	μm	435
Crude oil quality specifications		
Density at 15 °C	kg/m³	860
Water content	mg/kg	250

D5005 X-Ray Diffractometer using Ni-filtered CuKa (λ=0.154 nm) radiation at 45 kV and 40 mA and continuous scan mode. The XRD patterns were recorded in the scan range 2θ=5-70, at scan rate step=0.04 °, dwell time=3 sec, i.e. total scan time approximately 1 h and 30 min.

Following the technique proposed by Saeman *et al.* [35], the lignocellulosic materials were hydrolyzed to glucose and reducing sugars in nearly quantitative yields; the filtrates were analyzed for glucose using an enzymatic test and for reducing sugars using the Somogyi technique [36]. Based on these results the cellulose and hemicelluloses content of the adsorbents were estimated. Finally, the acid-insoluble lignin (Klason lignin) was determined according to the Tappi T222 om-88 method [37].

The concentration of Methylene Blue in the solution was obtained by measuring O.D. at 663 nm, using a HACH DR4000U UV–visible spectrophotometer.

The pH measurements were made using a digital pH meter, MultiLab model 540.
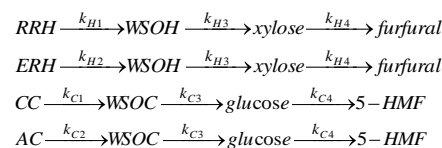
The water and oil adsorbency test, defined as the ratio of water or oil adsorbed to dry adsorbent weight, according to the ASTM F726-06 method [38], was performed, following the procedure of this standard method, using diesel 10 PPM produced by Hellenic Petroleum SA and crude oil. Quality specifications of diesel and crude oil are given in Table II.

3 RESULTS AND DISCUSSION

3.1. Autohydrolysis and maleic acid hydrolysis simulation.

Cellulose amorphous and crystalline fractions are hydrolyzed to water-soluble glucose, hemicelluloses are hydrolyzed mostly to xylose and the acid-insoluble lignin fraction is not affected by acid hydrolysis. The detailed simulation of (i) the autohydrolysis and (ii) the maleic acid hydrolysis process can be performed using simulation model described in earlier work [4].

The simulation model is presented below and concerns the hydrolysis of polysaccharides.

$$RRH \xrightarrow{k_{H1}} WSOH \xrightarrow{k_{H3}} xylose \xrightarrow{k_{H4}} furfural$$
$$ERH \xrightarrow{k_{H2}} WSOH \xrightarrow{k_{H3}} xylose \xrightarrow{k_{H4}} furfural$$
$$CC \xrightarrow{k_{C1}} WSOC \xrightarrow{k_{C3}} glucose \xrightarrow{k_{C4}} 5-HMF$$
$$AC \xrightarrow{k_{C2}} WSOC \xrightarrow{k_{C3}} glucose \xrightarrow{k_{C4}} 5-HMF$$

where: RRH is the Reaction Resisting Hemicelluloses; ERH the Easily Reacting Hemicelluloses; WSOH the Water Soluble Oligosaccharides from Hemicelluloses; CC the Crystalline Cellulose; AC the Amorphous Cellulose; WSOC the Water Soluble Oligosaccharides from Cellulose; 5-HMF the 5-hydroxymethyl furfural.

A system of first-order kinetic equations was applied to the hydrolysis of xylan 1 and xylan 2 (reaction-resisting and easily-reacting hemicelluloses, respectively) during the hydrolysis treatment. In that case, the maleic acid activity was assumed to be constant during the acid hydrolysis process (although decreasing slowly due to neutralization by the ash) while acid activity is changing during autohydrolysis due to production of organic acids [5]. Moreover, the hydrolysis of amorphous and crystalline cellulose, the hydrolysis of oligosaccharides and the degradation of xylose/glucose can all be simulated by first-order kinetic equations. The following equations simulated the hydrolysis reactions of the lignocellulosic materials:

$$-dC_{i1}/dt = k_{i1}.C_{i1} \tag{1}$$
$$-dC_{i2}/dt = k_{i2}.C_{i2} \tag{2}$$
$$dC_{i3}/dt = k_{i1}.C_{i1} + k_{i2}.C_{i2} - k_{i3}.C_{i3} \tag{3}$$
$$dC_{i4}/dt = k_{i3}.C_{i3} - k_{i4}.C_{i4} \tag{4}$$
$$k_{ij} = p_{ij} \cdot a \cdot e^{-E_{ij}/RT} \tag{5}$$

where $i=C$ for cellulose hydrolysis, $i=H$ for hemicelluloses hydrolysis, $j = 1, 2, 3,$ or 4; p_{ij} and E_{ij} are the pre-exponential factor (min⁻¹) and the activation energy (kJ/mol), respectively; a is the activity of the maleic acid or the organic acids produced by autohydrolysis and can be estimated by the equation $a = 10^{-pH}$ or $pH = -\log a$. The pH was measured at 25 °C at the end of the cooling period in each experiment. Eq. (5) is the well-known Arrhenius low. All concentration values C_{ij} ($i = C$ or H, $j = 1, 2, 3,$ or 4) in this model were expressed in w/w units, based on the initial quantity of dry components in the reacting system. The rate constants, k_{ij}, were expressed in min⁻¹, the reaction time t in min, and the reaction temperature T in K. ($C_{i1}+C_{i2}$) represents the concentration of the non-reacted polysaccharides (C_{i0}), and ($C_{i3}+C_{i4}$) represents the concentration of total sugars in the liquid phase (C_{iT}). The concentration of decomposition products (furfural, 5-HMF), C_{i5}, can be calculated from the expression 1-($C_{i0}+C_{iT}$). The concentrations of the hydrolysis soluble

products obtained from the polysaccharides (cellulose and hemicelluloses) are:

$$C_j = \frac{\sum\limits_{i=C,H} C_{i0,0} \cdot C_{ij}}{\sum\limits_{i=C,H} C_{i0,0}} \quad (j=0, 3, 4, T) \qquad (6)$$

where $C_{i0,0}$ is the initial experimental concentration of straw cellulose and hemicelluloses. The solid residue yield SRY (as a w/w fraction of initial dry material) is:

$$SRY = \sum_{i=C,H} C_{i0,0} \cdot C_{i0} + c \qquad (7)$$

where the constant c is independent of the reaction conditions and is equal to the acid insoluble components fraction. The quantity of the acid insoluble lignin (Klason) in the solid residue was constant and approximately equal to that in the original straw. The presented model can simulate the non-isothermal reaction system of polysaccharide (i) autohydrolysis and (ii) dilute maleic acid hydrolysis. It can also predict the concentration of polysaccharides under isothermal reaction conditions.

In the case of the autohydrolysis process, a severity factor [39, 40] is defined as

$$R_0 = \int_0^t e^{\frac{T_\theta - T_{r\theta}}{\omega}} \, dt \qquad (8)$$

where T_θ is temperature in °C (considered as a function of time in the batch reactor), t is the time in min, T_r (°C) is the reference temperature in °C, and ω an empirical parameter related with the activation energy, which can be expressed as

$$\omega = \frac{R \cdot T_r^2}{E_{H2}} \qquad (9)$$

where R = 0.0083 kJ/(mol·K) and E is the activation energy (kJ/mol). In this work, treatments were carried up to reach maximum temperatures in the range 140-180 °C. Assuming $T_{r\theta}$ = 100 °C or T_r = 373 K and E_{H2} = 104.0 kJ/mol, eq. (9) gives ω = 11.10 K [4]; numerical integration of Eq. (8) allowed the calculation of R_0 for each experiment. The R_0-model can be expressed as follows:

$$C_{i0} = D_i \cdot e^{-k_{i1} \cdot R_0} + (1 - D_i) \cdot e^{-k_{i2} \cdot R_0} \qquad (10)$$

where $i=C$ for cellulose, $i=H$ for hemicelluloses, D_i is the resisting to hydrolysis polysaccharide fraction (degree of crystallinity in the case of cellulose) and $L_{ijl} = k_{ij}/(k_{il} - k_{ij})$ ($i=C, H, j=1,2,3, l=3,4$). In fact, the R_0-model is similar to the isothermal model, in the case that R_0 plays the role of t and the effect of a is not taken into account.

In other cases, mostly in acid hydrolysis, a 'combined severity R_0'-factor' was introduced assuming isothermal reaction [41, 42] as follows

$$R_0' = 10^{-pH} \cdot t \cdot e^{\frac{T-100}{14.75}} \qquad [11]$$

In this work, as regards maleic acid hydrolysis, we introduced the following combined severity factor for non-isothermal reaction conditions

$$R_0^* = 10^{-pH} \cdot \int_0^t e^{\frac{T_\theta - 100}{11.10}}$$

or

$$\log R_0^* = -pH + \log \left(\int_0^t e^{\frac{T_\theta - 100}{11.10}} \right) \qquad (12)$$

As pH we used the average of the values of pH_{before}, i.e., pH measured before acid hydrolysis process and pH_{after}, i.e., pH measured after the hydrolysis pretreatment.

$$pH = \frac{pH_{before} + pH_{after}}{2} \qquad (13)$$

In this case, the solid residue yield y or SRY was estimated by the following simplified equation:

$$SRY = C_{0,0} e^{-p_\varphi \cdot \log R_0^*} + c \qquad (14)$$

where $C_{0,0}$ stands for the initial polysaccharides percentage of wheat straw, p_φ represents a phenomenological depolymerization kinetic constant and c is a constant equal to the acid insoluble components fraction (independent of the reaction conditions).

3.2. Design of Experiments (DOE)

In the following analysis a Design of Experiments (DOE) approach was conducted in order to examine the effects of experimental conditions on the reaction system pH, the SRY and the modified wheat straw adsorptivity. When performing an experiment, varying the levels of the factors ($C_4H_4O_4$ concentration in M, temperature in °C and isothermal reaction time in min) simultaneously rather than one at a time is efficient in terms of time and cost, and also allows the study of linear and square effects of the factors and interactions between them in the experiment responses (the reaction system pH, the SRY and the modified wheat straw adsorptivity). A three level Box-Behnken design was chosen, with three center points to check for curvature in the response surface. The factor levels are displayed in Table III.

The design table for the modification of wheat straw by maleic acid hydrolysis is presented below (Table IV), where "StdOrder" shows what the order of the runs in the experiment would be if it was done in standard order and "RunOrder" shows what the order of the runs in the experiment would be in random order. This

Table III: DOE factor levels.

Factors	Factor levels			Units
	-1	0	1	
$C_4H_4O_4$ Concentration, C	0.01	0.05	0.09	M
Temperature, T	140	160	180	°C
Reaction time, t	0	25	50	min

**Table IV:** Experimental design for the modification of wheat straw by maleic acid hydrolysis.

StdOrder	RunOrder	PtType	Blocks	Maleic acid concentration (M)	T (°C)	t (min)	Preheating time (min)	Total time (min)
2	1	2	1	0.09	140	25	35	60
7	2	2	1	0.01	160	50	42	92
4	3	2	1	0.09	180	25	50	75
6	4	2	1	0.09	160	0	42	42
5	5	2	1	0.01	160	0	42	42
8	6	2	1	0.09	160	50	42	92
10	7	2	1	0.05	180	0	50	50
3	8	2	1	0.01	180	25	50	75
11	9	2	1	0.05	140	50	35	85
13	10	0	1	0.05	160	25	42	67
12	11	2	1	0.05	180	50	50	100
1	12	2	1	0.01	140	25	35	60
14	13	0	1	0.05	160	25	42	67
15	14	0	1	0.05	160	25	42	67
9	15	2	1	0.05	140	0	35	35

randomization of the order reduces the chance that differences in experimental materials or conditions strongly bias results and allows the estimation of the inherent conditions in order to make valid statistical inferences based on the experimental data. "PtType" refers to the type of point in the designed experiment, where 0 is the center point and 2 the edge midpoint. The experimental runs were conducted under relatively homogeneous conditions ("Block"=1).

It must be mentioned that 'Total time' = 'Preheating time' + t, where t is the isothermal time of the reaction. In the DOE analysis, coded units were used in order to compare the size of the coefficients and the impact on the response as well as estimate the model terms independently. The Analysis of variance for the response variables shows that pH before and after, they are strong functions of maleic acid concentration C, in its square form and the interaction of C with the temperature T ($p < 0.05$). Also, SRY is a strong function of all the factors, their interactions and C in its square form as well, with high statistical significance ($p < 0.001$).

3.3. Maleic acid hydrolysis results

For the case of maleic acid hydrolysis, the temperature profiles are given in Fig. 1 while the pH profile is presented in Fig. 2; the values of pH_{before}, i.e., pH measured before acid hydrolysis process and pH_{after}, i.e., pH measured after the hydrolysis pretreatment are shown. The maleic acid hydrolysis solid-residue yield vs. the new Severity Factor (calculated in Table V) is
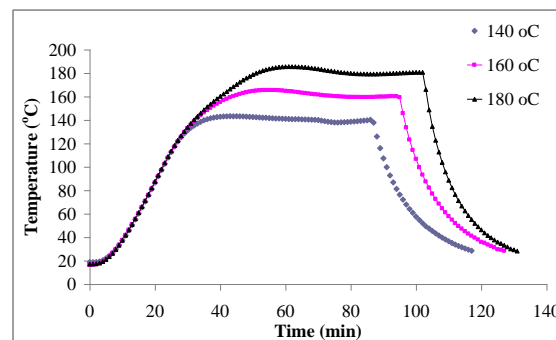
Figure 1: Maleic acid hydrolysis temperature profiles for isothermal reaction time t=50 min.
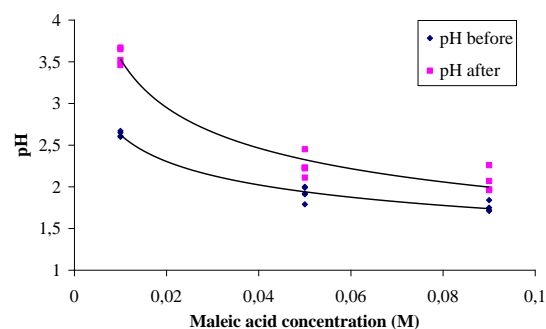
Figure 2: Maleic acid hydrolysis pH vs. acid concentration.
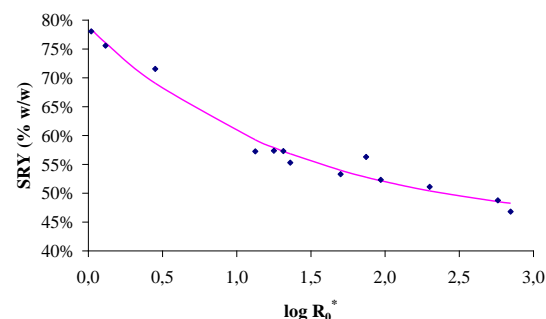
Figure 3: Maleic acid hydrolysis solid-residue yield vs. Severity Factor.

shown in Fig. 3. The theoretical curves were simulated according to the above model eq. (14).

On the other hand, the above described DOE analysis generates the following models (in uncoded-physical units) presented in Figs. 4-6.

3.4. BET surface area

The BET surface area of the maleic acid hydrolyzed wheat straw is given in Fig. 7 vs. the severity factor. It is given by the following equation

$$y = -0.6553x^2 + 3.6987x + 1.0379, \quad 0 < x < 3 \qquad (15)$$

where y = BET surface area in m^2/g, x = $\log R_0^*$ while the coefficient of determination R^2 is 0.8244. The BET surface area of the untreated wheat straw was 0.374 m^2/g while the BET surface for the maleic acid treated material reaches the 6.42 m^2/g.

Table V: Severity factor values for the modification of wheat straw by maleic acid hydrolysis.

Maleic acid concentration (M)	T (°C)	t (min)	R_0	R_0^*	$\log R_0^*$
0.01	140	25	1426.9	1.05	0.019
0.01	160	0	1844.2	1.31	0.116
0.05	140	0	292.3	2.82	0.451
0.01	160	50	15494.2	13.34	1.125
0.05	140	50	2293.1	17.80	1.250
0.09	140	25	1426.9	20.63	1.314
0.09	160	0	1844.2	22.95	1.361
0.01	180	25	58237.6	50.14	1.700
0.05	160	25	9602.0	74.54	1.872
0.05	180	0	10993.2	93.57	1.971
0.09	160	50	15494.2	199.60	2.300
0.09	180	25	58237.6	575.71	2.760
0.05	180	50	92518.2	701.82	2.846
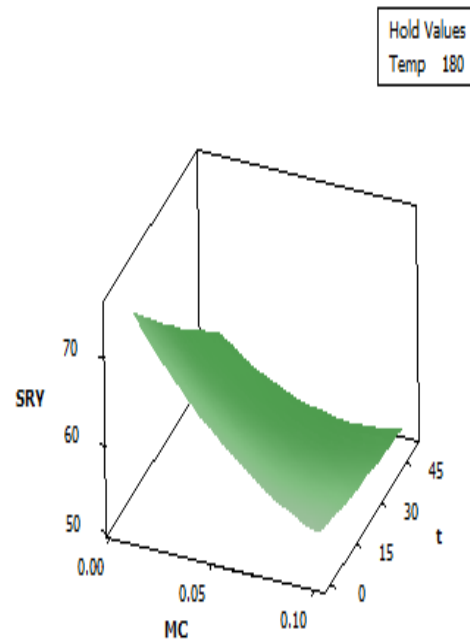
Figure 5: Surface plots of maleic acid concentration (MA) and time (*t*) effect on maleic acid hydrolysis solid-residue yield SRY.
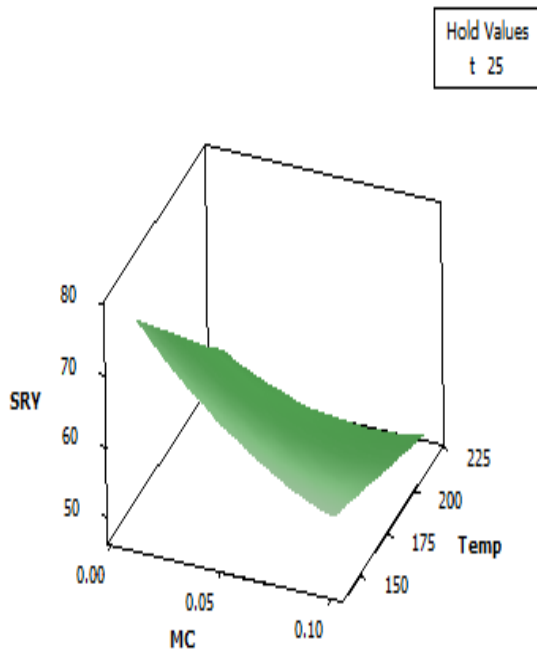
Figure 4: Surface plots of maleic acid concentration (MC) and temperature (Temp) effect on maleic acid hydrolysis solid-residue yield SRY.
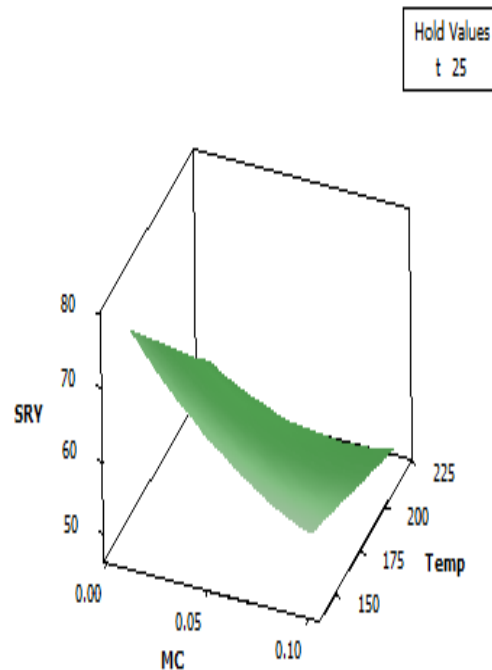
Figure 6: Surface plots of maleic acid concentration (MA) and temperature (Temp) effect on maleic acid hydrolysis solid-residue yield SRY.
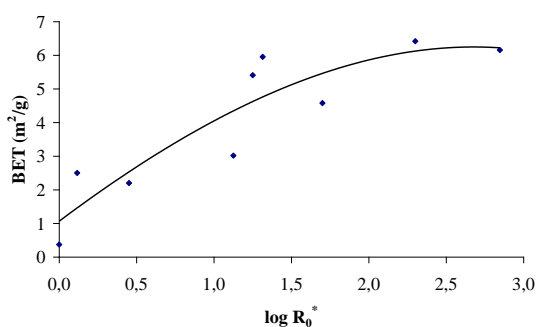
Figure 7: BET surface of the maleic acid hydrolyzed wheat straw vs. severity factor.

Lignin of the untreated straw remained practically untouched by the autohydrolysis and acid hydrolysis pretreatment. The removal of the hemicelluloses, the amorphous cellulose and part of the crystalline cellulose, and the swelling of the crystalline cellulose fraction results in 'opening' of the structure of the lignocellulosic matrix and the increasing of the BET surface area, which possibly accounts for the advanced adsorption properties of the pretreated materials over the untreated ones. In addition, the pretreatment of the material leads to the activation of the internal surface of straw particles, thus increasing the number of active sites available for basic dye binding [5].

3.5 XRD patterns

The XRD patterns of the untreated and the maleic acid hydrolyzed (0.05 M, 180 ^{o}C, 50 min) wheat straw are given in Fig. 8. The remaining cellulose has enhanced crystallinity index comparing to the cellulose of the nitrated wheat straw.
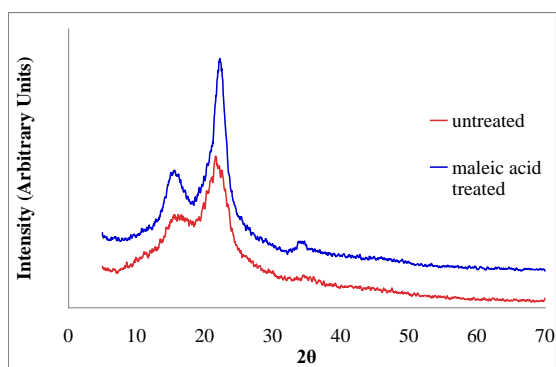

Figure 8: XRD patterns of the untreated and the maleic acid hydrolyzed (0.05 M, 180 ^{o}C, 50 min) wheat straw.

The straw particles mainly consist of cellulose and lignin, and many hydroxyl-rich compounds, such as tannins or other phenolic compounds. All these components exhibit properties contributing to ion exchange, which is a significant stage in several kinds of adsorption, favoring also some penetration of the adsorbate beyond the surface of the adsorbent. Since ion exchange is combined to adsorption, studies in particular kinetics and isotherms, provide information on the mechanism of sorption. These mechanisms are, in general, complicated because they implicate the presence

of different interactions. In addition, a wide range of chemical structures, pH, salt concentrations and the presence of ligands often add to the complication. Some of the reported interactions include: ion-exchange, complexation, coordination / chelation, electrostatic interactions, acid–base interactions, hydrogen bonding, hydrophobic interactions, physical adsorption, precipitation [5].

3.6 SEM micrographs.

In Fig. 9 and 10 the SEM micrographs for mild (0.01 M maleic acid at 140 ^{o}C for 0 min) and severe (0.05 M maleic acid at 180 ^{o}C for 30 min) modified wheat straw are presented. The destruction of the lignocellulosic matrix is obvious at severe conditions.

3.7 Adsorption isotherms

The comparison of the adsorption capacity of the untreated and pretreated straw samples was based on the Freundlich [43], Langmuir [44] and many other isotherm models. The first two models are both widely used for investigating the adsorption of a plethora of dyes on various lignocellulosic materials and activated carbons. The Freundlich [43] isotherm is given by the following equation:

$$q = K_F \cdot (C_e)^{\frac{1}{n}} \qquad (16)$$

where q is the amount adsorbed per unit mass of the adsorbent (mg/g), C_e is the equilibrium concentration of the adsorbate (mg/L) and K_F, n are the Freundlich constants related to adsorption capacity and intensity, respectively. Deriving the logarithmic form of eq. (16):

$$\log q = \log K_F + \frac{1}{n} \log C_e \qquad (17)$$

The Freundlich constants K_F and n were estimated by non-linear regression analysis (by using the estimates of the linearized regression model eq. (17) as initial guesses) from the experimental adsorption data obtained at 23^{0}C for Methylene Blue.

Fig. 11 presents, as a basic dye example, Methylene Blue adsorption isotherms by untreated and maleic acid treated wheat straw (pretreatment with 0.01 M maleic acid, at 200 ^{o}C for 10 min isothermal + preheating time period). The theoretical curves are estimated according to the Freundlich equation. The Freundlich parameter values are shown in Table VI. The K_F values estimated for the autohydrolysis-treated samples were significantly higher comparing to those of the untreated material, indicating an increased adsorption capacity of the former. The parameter n was not significantly affected by the pretreatment conditions. The standard error of estimates (SEE)-values were calculated by the following equation

$$SEE = \sqrt{\sum_{i=1}^{n'} (y_i - y_{i,theor})^2 / (n'-p')} \qquad (18)$$

where: y_i is the experimental value of the depended variable, $y_{i,theor}$ is the theoretical (estimated) value of the depended variable, n' is the number of the experimental measurements and p' is the number of parameters, i.e., $(n'-p')$ is the number of the degrees of freedom.

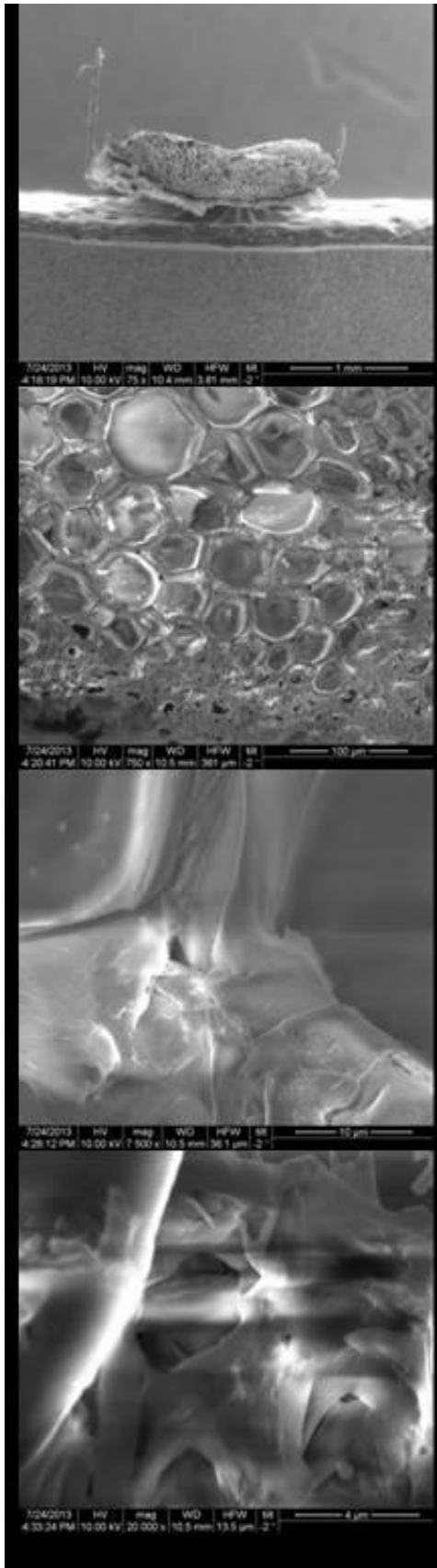The Langmuir isotherm equation [44] is based on the following 'pseudo-monolayer' adsorption model.

Figure 9: SEM images of wheat straw modified by maleic acid 0.01 M at 140 °C for 0 min. Cross section with magnifications X75, X750, X7,500 and X20,000 (increasing top-down).
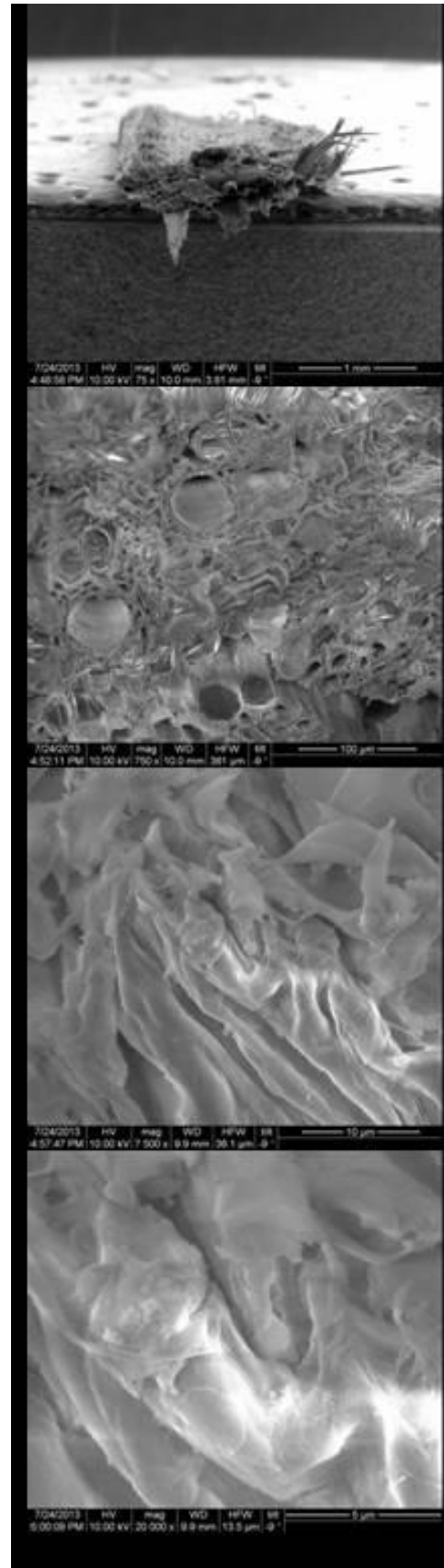

Figure 10: SEM images of wheat straw modified by maleic acid 0.05 M at 180 °C for 30 min. Cross section with magnifications X75, X750, X7,500 and X20,000 (increasing top-down).
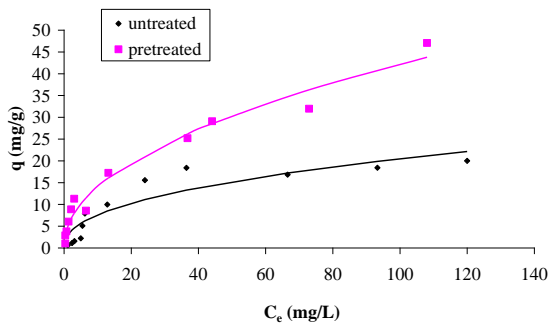
Figure 11: Freundlich isotherms for MB adsorption on untreated and pretreated (maleic acid 0.01 M, 160 $^\circ$C, 0 min isothermal time) wheat straw.

Table VI: Parameters of the Freundlich isotherms for MB adsorption on untreated and pretreated (maleic acid 0.01 $^\circ$C, 160 $^\circ$C, 0 min isothermal time) wheat straw.

	Linear regression analysis		Non linear regression analysis	
	untreated	pretreated	untreated	pretreated
K_F	0.90	4.04	2.83	4.68
n	1.33	1.89	2.33	2.09
R	0.9262	0.9522		
SEE			3.07	1.66

$$q = \frac{K_L q_m C_e}{1 + K_L C_e} \qquad (19)$$

which may give the linearized form

$$\frac{1}{q} = \left(\frac{1}{q_m}\right) + \left(\frac{1}{K_L \cdot q_m}\right) \cdot \left(\frac{1}{C_e}\right) \qquad (20)$$

where K_L is the Langmuir constant related to the energy of adsorption (L.mg^{-1}) and q_m the amount of dye adsorbed (mg.g^{-1}) when saturation is attained. In cases where the isotherm experimental data approximates the Langmuir equation, the values of the parameters K_L and q_m can be estimated either by plotting $1/q$ versus $1/C_e$ either by non-linear regression analysis.

In case that the Langmuir model is well fitted to data, the essential characteristics of the adsorption isotherm can be described by a dimensionless constant called 'equilibrium parameter' or 'separation factor' R_L, defined by the following equation:

$$R_L = \frac{1}{1 + K_L \cdot C_0} \qquad (21)$$

where C_0 is the initial dye concentration (mg/L) and K_L is the Langmuir constant (L/mg). The value of R_L indicates the type of the adsorption isotherm to be either unfavorable ($R_L > 1$), linear ($R_L = 1$), favorable ($0 < R_L < 1$) or irreversible ($R_L = 0$). At the present work, the R_L values confirmed that the wheat straw is favorable for

adsorption of dye or heavy metal under optimal conditions used in this study.

The Sips (Langmuir – Freundlich) [45] isotherm equation, also examined in the present work, is based on the following adsorption model.

$$q = \frac{q_m \cdot \left(K_L \cdot C_e\right)^{1/n}}{1 + \left(K_L \cdot C_e\right)^{1/n}} \qquad (22)$$

where K_L is the Langmuir constant (L/mg), q_m the amount of dye adsorbed (mg/g) when the saturation is attained, and n the Freundlich constant.

The Radke–Prausnitz [46] isotherm equation, also called by some authors as Fritz–Schluender isotherm equation, is based on the following adsorption model.

$$q = \frac{K_L \cdot q_m \cdot C_e}{1 + K_L \cdot C_e^{1/n}} \qquad (23)$$

where K_L is the Langmuir constant (L/mg), q_m the amount of dye adsorbed (mg/g) when the saturation is attained, and n the Freundlich constant. Moreover, the Redlich – Peterson isotherm equation

$$q = \frac{K_R \cdot C_e}{1 + a_R \cdot C_e^{\beta}} \qquad (24)$$

can be transformed to the Radke – Prausnitz isotherm by substituting $K_R = K_L \cdot q_m$, $a_R = K_L$ and $\beta = 1/n$.

The Modified Radke – Prausnitz [47] isotherm equation is based on the following adsorption model.

$$q = \frac{K_L \cdot q_m \cdot C_e}{\left(1 + K_L \cdot C_e\right)^{1/n}} \qquad (25)$$

where K_L is the Langmuir constant (L/mg), q_m the amount of dye adsorbed (mg/g) when the saturation is attained, and n the Freundlich constant.

The Tóth [48] isotherm equation is based on the following adsorption model.

$$q = \frac{q_m \cdot C_e}{\left(1/K_L + C_e^n\right)^{1/n}} \qquad (26)$$

where K_L is the Langmuir constant (L/mg), q_m the amount of dye adsorbed (mg/g) when the saturation is attained, and n the Freundlich constant.

The UNILAN isotherm equation is based on the following adsorption model.

$$q = \frac{q_m}{2s} \ln\left(\frac{1 + K_L \cdot C_e \cdot e^s}{1 + K_L \cdot C_e \cdot e^{-s}}\right) \qquad (27)$$

where K_L is the Langmuir constant (L/mg), q_m the amount of dye adsorbed (mg/g) when the saturation is attained, and s a constant.

The Temkin isotherm model [49] is

$$q = \frac{RT}{b_T} \ln(A_T C_e) \ \text{ or } \ q = B_T \ln(A_T C_e)$$

or $q = q_m \ln(K_L C_e)$ (28)

where R=0.008314 kJ mol^{-1} K^{-1}, T is the adsorption temperature in K, K_L=A_T in L mg^{-1} and q_m=B_T=RT/b_T in mg g^{-1}. In linearized form Eq (24) is as follows

$q = a_T + q_m \ln(C_e)$ (29)

where a_T=$q_m \ln(K_L)$.

The Dubinin-Radushkevich [50] isotherm model is

$$q = q_D \exp\{-B_D[RT\ln(1+\frac{1}{C_e})]^2\} \text{ or}$$

$$q = q_D \exp\{-A_D[\ln(1+\frac{1}{C_e})]^2\} \text{ or}$$

$$q = q_m \exp\{-n[\ln(1+\frac{1}{C_e})]^2\}$$ (30)

where q_m=q_D in mg g^{-1} and n=A_D=$B_D R^2 T^2$ a dimensionless constant for T=constant. The parameters of the nine isotherm models can be obtained by non-linear regression analysis (NLRA).

3.8 Kinetics of adsorption

The kinetics of adsorption of Methylene Blue and Cr(VI) on several lignocellulosic materials has been extensively studied using various kinetic equations. At first place, we used Lagergren equation [51]:

$q - q_t = q \cdot e^{-k \cdot t}$ (31)

where q and q_t are the amounts of dye adsorbed per unit mass of the adsorbent (in mg/g) at equilibrium time ($t \to \infty$) and adsorption time t, respectively, while k is the pseudo-first order rate constant for the adsorption process (in min^{-1}). Moreover, $q=(C_0 - C_e)V/m$ and $q_t = (C_0 - C)V/m$, where C, C_0, C_e are the concentrations of methylene blue in the bulk solution at time t, 0, and ∞, respectively, while m is the weight of the adsorbent used (in g), and V is the solution volume (in mL). Further modification of eq. (31) in logarithmic form gives:

$\ln(q - q_t) = \ln q - k \cdot t$ (32)

The plots of $\ln(q - q_t)$ vs. t for MB and Cr(VI) adsorbent systems were found to be linear, indicating the possibility of first order nature of the adsorption process. MB and Cr(VI) adsorption kinetics by untreated and pretreated (autohydrolysis at 200 °C for 10 min) wheat straw are presented in Fig. 12. The theoretical curves are estimated according to the Lagergren equation by means of NLRA. All *SEE*-values were found satisfactorily low, indicating the applicability of this kinetic equation to the adsorption of MB on wheat straw (see Table VII).

According to the Lagergren model and the Arrhenius law $k = p \cdot \exp(-E/RT)$, the activation energy for the adsorption of MB on untreated and pretreated wheat straw was estimated by linear regression of ln$k$ (rate constant k in min^{-1}) on $1/T$ (T in K). The Methylene Blue adsorption activation energy E was found to be 14-15 kJ/mol for the treated materials, approximately equal to the activation energy of the untreated material (15
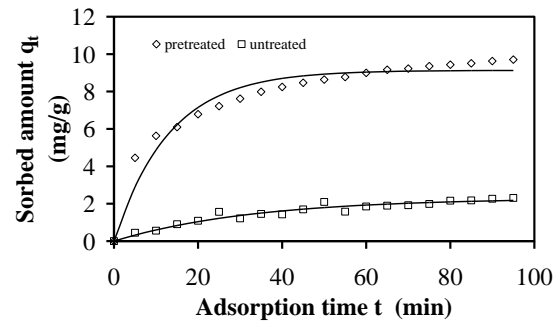

Figure 12: Lagergren kinetics for MB adsorption on untreated and pretreated (maleic acid 0.01 M, 160 °C, 50 min isothermal time) wheat straw for pH=8.

Table VII: Parameters of the Lagergren kinetic equation for MB adsorption on untreated and pretreated (maleic acid 0.01 M, 160 °C, 50 min isothermal time) wheat straw for pH=8.

	untreated	pretreated
k (min^{-1})	0.0300	0.0763
q (mg/g)	2.31	9.13
SEE	0.1574	0.5524

kJ/mol). This indicates that a physical process, i.e. the intra-particle diffusion, is the controlling step of the adsorption process. Assuming a κ-order kinetic model:

$dq/dt = k (q - q_t)^\kappa$ (33)

From the differential eq. 33 for $\kappa \neq 1$ we obtain:

$q_t = q - [q^{1-\kappa} + (\kappa-1)kt]^{1/(1-\kappa)}$ (34)

The order of the kinetic model was found to be around 2 for untreated and pretreated material. For κ=2, the pseudo-second order kinetic model [52] obtained is the following

$q_t = q - [q^{-1} + kt]^{-1}$ or $q_t = q - \dfrac{1}{\dfrac{1}{q}+kt}$ (35)

The values of the second order rate constants were estimated by NLRA. All *SEE*-values were found low.

Agitation is an important parameter in sorption phenomena, influencing the distribution of the solute in the bulk solution and the formation of the external boundary film. The effect of stirring speed (in rpm) on the adsorption rate constant k (in min^{-1}) of the untreated material was investigated. The kinetics seemed to be affected by the agitation speed for values between 0 - 200 rpm, thus confirming that the influence of external diffusion on the sorption kinetic control plays a significant role. In contrast, the small effect of agitation in the range of 200 - 600 rpm showed that external mass transfer was not the rate limiting step, and implied that intraparticle diffusion resistance needed to be included in the analysis of overall sorption [5].

The effect of the pH of the MB dye solution on the amount of dye adsorbed was studied by varying the initial

pH under constant process parameters. The final concentration C of dyes solutions after an adsorption period of 190 min was significantly higher for pH values between 1.5 – 4 for both untreated and pretreated materials than the relevant concentration (C for $t = 190$ min) for pH = 8. The lower adsorption of dye at acidic pH was due to the presence of excess H^+ ions that competed with the dye cation for adsorption sites. As the pH of the system increased (pH > 8), the number of positively charged available sites decreased while the number of the negatively charged sites increased. The negatively charged sites favored the adsorption of dye cation due to electrostatic attraction. The increase in initial pH from 8 to 13, slightly increased the amount of dye adsorbed. The final pH of the solution was found to decrease only slightly (by 0.3 – 0.5 pH units) after adsorption of dye with the release of H^+ ions from the active site of the adsorbent surface. The results were in agreement with other literature reports [5].

Adsorbate species are probably transported from the bulk of the solution into the solid phase through an intra-particle diffusion/transport process, which is frequently the rate-limiting step in many adsorption processes, especially in a rapidly stirred batch reactor. The possibility of intra-particle diffusion was explored by using the intra-particle diffusion model [36]:

$$q_t = k_p \cdot \sqrt{t} \qquad (36)$$

where q_t is the amount of dye adsorbed at time t and k_p is the intra-particle diffusion rate constant in $mg \cdot g^{-1} \cdot min^{-0.5}$. In the case of Methylene Blue, the values of the intra-particle diffusion model rate constants k_p were estimated by NLRA.

3.9 Oil spills cleaning by adsorption on untreated and modified wheat straw.

Modified wheat straw was used for the adsorption of hydrocarbons (diesel and crude oil) [53]. The modification was achieved using autohydrolysis and maleic acid hydrolysis as pretreatment processes. In the case of maleic acid hydrolysis, the water, diesel and crude oil adsorptivity results of untreated and maleic acid pretreated wheat straw are presented in Figs. 13 and 14 vs. the severity factor. Optimal pretreatment conditions, with maximum adsorptivity values, were observed for log $R_0^* = 1.7$, i.e., 0.01 M maleic acid, 180 ^{o}C for 25 min (without including preheating time).
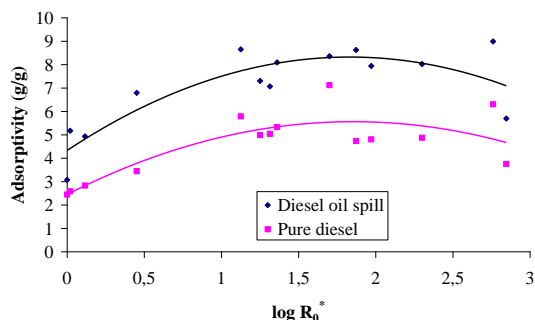

Figure 13: Diesel adsorbency vs. the severity factor for maleic acid modified wheat straw.
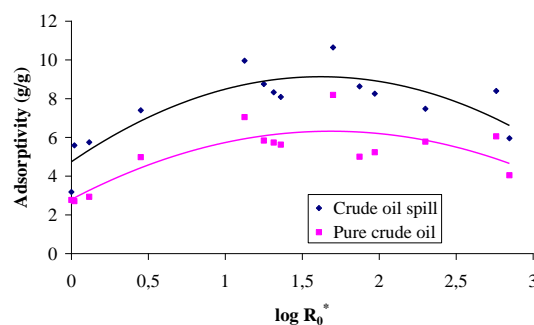

Figure 14: Crude oil adsorbency vs. the severity factor for maleic acid modified wheat straw.

As regards the diesel adsorbency of the maleic acid hydrolyzed wheat straw (Fig. 13), in the case of pure diesel the adsorptivity is given by the following equation

$$y = -0,9051x^2 + 3,3549x + 2,4516 \qquad (37)$$

where y = diesel adsorbency in g/g, x = log R_0^* and coefficient of determination $R^2 = 0,6952$. In the case of diesel oil spill on water the adsorptivity is given by the following equation

$$y = -1,1912x^2 + 4,3612x + 4,3319 \qquad (38)$$

where y = diesel adsorbency in g/g, x = log R_0^* and $R^2 = 0,7477$.

As regards the crude oil adsorbency of the maleic acid hydrolyzed wheat straw (Fig. 14), in the case of pure crude oil the adsorptivity is given by the following equation

$$y = -1,2373x^2 + 4,1737x + 2,7975 \qquad (39)$$

where y = crude oil adsorbency in g/g, x = log R_0^* and coefficient of determination $R^2 = 0,6944$. In the case of crude oil spill on water the adsorptivity is given by the following equation

$$y = -1,6738x^2 + 5,422x + 4,7413 \qquad (40)$$

where y = crude oil adsorbency in g/g, x = log R_0^* and $R^2 = 0,7439$.

In the case of maleic acid hydrolysis, diesel and crude oil adsorptivity results of untreated and maleic acid hydrolysis-pretreated wheat straw are compared to the most commonly used commercial adsorbents in Table VIII.

As regards field-simulation of oil spills cleaning, field-water sampling locations were selected (in cooperation with the Hellenic Center for Marine Research - HCMR) as follows: two ports for seawater (ΛΣ = Skaramagas Port and ΛΠ = Piraeus Port), one lake (ΛΚ = Koumoundourou Lake), and one stream (P6 = Pikrodafnis Stream). The map of these locations is presented in Fig. 15. The water sampling dates covered from 8 January 2013 to 18 January 2014. The wheat straw used herein for adsorbent was harvested during 2012 and modified by autohydrolysis at optimal conditions (200 ^{o}C, 10 min isothermal time + preheating period) during 2013.

Table VIII. Diesel and crude oil adsorbency of untreated and modified (by maleic acid hydrolysis) wheat straw vs. the most commonly used commercial adsorbents.

Oil	Sorbents	Adsorbency (g/g)
Crude oil	Oil adsorbent pad	12.21
	Oil adsorbent pom poms	5.06
	Untreated wheat straw	2.45
	Pretreated wheat straw	7.12
Diesel	Oil adsorbent pad	10.26
	Oil adsorbent pom poms	3.68
	Untreated wheat straw	2.77
	Pretreated wheat straw	8.19

Figure 15: Field-water sampling locations (two ports for seawater, one lake and one stream): ΛΣ = Skaramaga Port, ΛΚ = Koumoundourou Lake, ΛΠ = Piraeus Port, and P6 = Pikrodafnis Stream. Sampling period: 8 January 2013 to 18 January 2014.
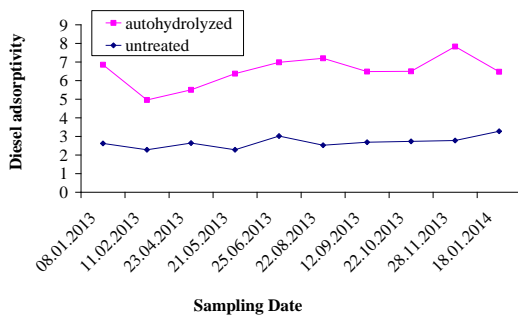
Figure 16: Diesel adsorption on untreated and pretreated (autohydrolysis 200 °C, 10 min isothermal time) wheat straw; oil spill on Piraeus Port.
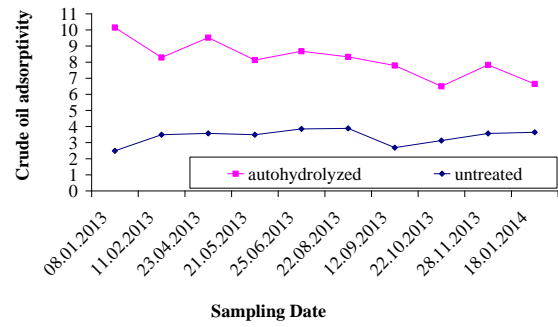

Figure 17: Crude oil adsorption on untreated and pretreated (autohydrolysis 200 °C, 10 min isothermal time) wheat straw; oil spill on Piraeus Port.

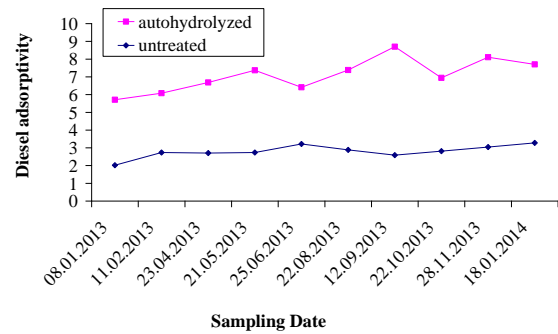**Figure 18:** Diesel adsorption on untreated and pretreated (autohydrolysis 200 °C, 10 min isothermal time) wheat straw; oil spill on Skaramaga Port.
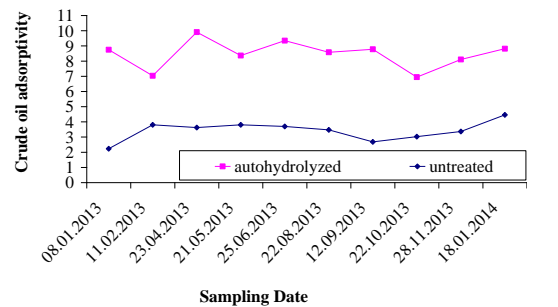

Figure 19: Crude oil adsorption on untreated and pretreated (autohydrolysis 200 °C, 10 min isothermal time) wheat straw; oil spill on Skaramaga Port.
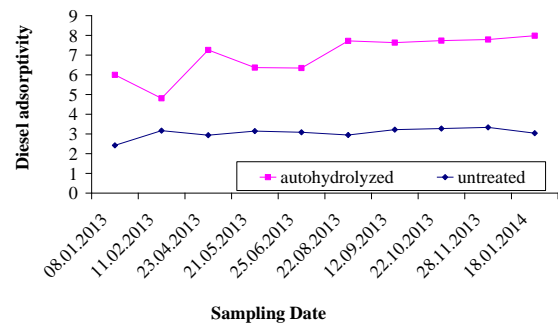

Figure 20: Diesel adsorption on untreated and pretreated (autohydrolysis 200 °C, 10 min isothermal time) wheat straw; oil spill on Pikrodafnis stream.
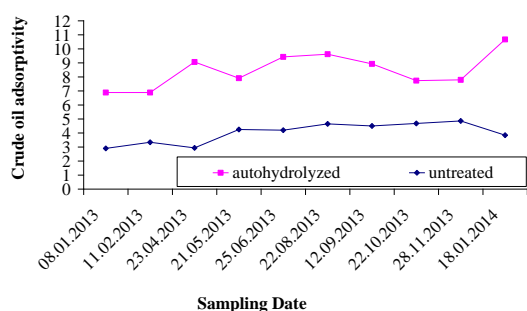
Figure 21: Crude oil adsorption on untreated and pretreated (autohydrolysis 200 °C, 10 min isothermal time) wheat straw; oil spill on Pikrodafnis stream.
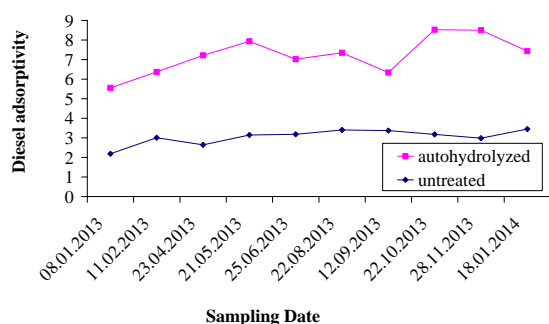

Figure 22: Diesel adsorption on untreated and pretreated (autohydrolysis 200 °C, 10 min isothermal time) wheat straw; oil spill on Koumoundourou Lake.
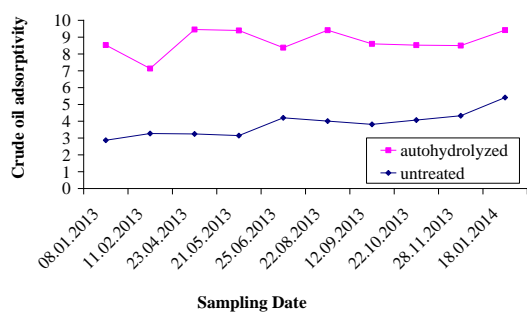

Figure 23: Crude oil adsorption on untreated and pretreated (autohydrolysis 200 °C, 10 min isothermal time) wheat straw; oil spill on Koumoundourou Lake.

The diesel and crude oil adsorbencies of untreated and pretreated (autohydrolyzed at 200 °C for 10 min) wheat straw are presented in Figs. 16-23, for oil spills on seawater (two Ports), stream water and lake water. The diesel and crude oil adsorptivity of the pretreated material is significantly enhanced comparing to that of the untreated one. As regards the sampling period 8 January 2013 to 18 January 2014, the average diesel and crude oil adsorptivities of untreated and autohydrolyzed wheat straw are presented in Table IX for oil spills on Piraeus Port, Skaramagas Port, Pikrodafnis stream and Koumoundourou Lake water.

Table IX: Diesel and crude oil adsorptivity (in g/g) of untreated and autohydrolyzed (200 °C, 10 min) wheat straw; oil spills on Piraeus Port, Skaramagas Port, Pikrodafnis stream and Koumoundourou Lake water; sampling period: 8 January 2013 to 18 January 2014.

	diesel oil spill		crude oil spill	
	Auto-hydro-lyzed	untreated	Auto-hydro-lyzed	untreated
Piraeus Port				
Average	6.51	2.70	8.18	3.43
St. dev.	0.82	0.32	1.13	0.47
Error %	13%	12%	14%	14%
Skaramagas Port				
Average	7.11	2.84	8.46	3.44
St. dev.	0.93	0.38	0.92	0.62
Error %	13%	13%	11%	18%
Pikrodafnis stream				
Average	6.96	3.13	8.49	3.97
St. dev.	1.04	0.40	1.25	0.70
Error %	15%	13%	15%	18%
Koumoundourou Lake				
Average	7.22	3.14	8.73	3.83
St. dev.	0.96	0.50	0.72	0.75
Error %	13%	16%	8%	19%

Autohydrolyzed and acid hydrolyzed wheat and barley straw could be made widely available for use as an alternative to commercial adsorbents for the removal of basic dyes, heavy metals and hydrocarbons from water/wastewater effluents and oil spills. Furthermore, as straw is an industrial waste and no addition of chemicals is required (especially in the case of autohydrolysis), we argue that this process of adsorbent modification may be considered to take place within an 'Industrial Ecology' framework, since a (solid) waste is used to treat another (aquatic) waste, contributing to pollution abatement without entailing excessive cost. This is an argument *a fortiori*, when additives (e.g., acids, salts, solvents etc) are used to enhance adsorptivity on condition they are available in the vicinity as waste or low value by-products of proper quality [5].

4   CONCLUSIONS

Experimental design for the maleic acid treatment of wheat straw was carried out. The kind of the waste-based lignocellulosic adsorbent examined herein was selected by means of multicriteria analysis and subsequently studied with a view to correlating its adsorptivity with surface topography and chemical composition. The SEM images, the BET surface area and the XRD patterns for untreated and maleic acid modified wheat straw were studied. A new severity factor $\log R_0^*$ was developed to incorporate the effect of maleic acid concentration, hydrolysis temperature and isothermal reaction time. Optimal modification conditions were found to maximize

the diesel and the crude oil adsorptivity of maleic acid treated wheat straw. Moreover, diesel oil spills were formed on seawater (two Ports), stream water and lake water for the sampling period 2013-2014. The diesel and crude oil adsorption on untreated and autohydrolyzed wheat straw was measured. The diesel and crude oil adsorption on autohydrolyzed wheat straw was significantly higher compared to that of the untreated material.

5 REFERENCES

[1] Srinivasan, A., Viraraghavan, T., 2008. Removal of oil by walnut shell media. Bioresour. Technol. 99(17), 8217-8220.

[2] Sidiras D., Konstantinou I.. Modification of barley straw by acid hydrolysis to be used as diesel and crude oil adsorbent. 20th European Biomass Conference and Exhibition - Setting the course for a biobased economy. Milan, Italy. 18-22 June 2012. pp. 1158-1163

[3] Sidiras D.K., Konstantinou I.G., Politi T.K.. Autohydrolysis Modified Barley Straw as Low Cost Adsorbent for Oil Spill Cleaning. 19th European Biomass Conference and Exhibition", Berlin 6-10 June 2011, pp. 1810-1815.

[4] Sidiras, D., Batzias, F., Ranjan, R., Tsapatsis, M., 2011. Simulation and optimization of batch autohydrolysis of wheat straw to monosaccharides and oligosaccharides. Bioresour. Technol. 102, 10486–10492.

[5] Sidiras, D., Batzias, F., Schroeder, E., Ranjan, R., Tsapatsis, M., 2011. Dye adsorption on autohydrolyzed straw in batch and fixed-bed systems. Chem. Eng. J. 171(3), 883-896.

[6] Sidiras, D., Bountri, A., Konstantinou, I., Batzias, F. On the validity of the Law of diminishing returns in packed bed columns used for wastewater treatment. Recent Researches in Energy and Environment. 6th IASME/WSEAS International Conference on Energy and Environment, EE'11, Cambridge, UK, February 23-25, 2011, pp. 160-165.

[7] Batzias, F.A., Sidiras, D.K., 2007. Simulation of methylene blue adsorption by salts-treated beech straw in batch and fixed-bed systems. J. Hazard. Mater. 149, 8-17.

[8] Batzias, F.A., Sidiras, D.K., 2007. Dye adsorption by prehydrolysed beech straw in batch and fixed-bed systems. Bioresour. Technol. 98, 1208-1217.

[9] Batzias, F., Sidiras, D., Schroeder, E., Weber, C., 2009. Simulation of dye adsorption on hydrolyzed wheat straw in batch and fixed-bed systems. Chem. Eng. J. 148, 459-472.

[10] Witka-Jezewska, E., Hupka, J., Pieniazek, P., 2003. Investigation of oleophilic nature of straw sorbent conditioned in water. Spill Science & Technology Bulletin 8(5-6), 561-564.

[11] Khan, E., Virojnagud, W., Ratpukdi, T., 2004. Use of biomass sorbents for oil removal from gas station runoff. Chemosphere 57(7), 681-689.

[12] Said, A.E-A.A., Ludwick, A.G., Aglan, H.A., 2009. Usefulness of raw bagasse for oil absorption: A comparison of raw and acylated bagasse and their components. Bioresour. Technol. 100(7), 2219-2222.

[13] Husseien, M., Amer, A.A., El- Maghraby, A., Taha, N.A., 2008b. Experimental Investigation of Thermal Modification Influence on Sorption Qualities of Barley Straw. Journal of Applied Sciences Research 4 (6), 652-657.

[14] Sun, X.F., Sun, R.C., Sun, J.X., 2004a. Acetylation of sugarcane bagasse using NBS as a catalyst under mild reaction conditions for the production of oil sorption-active materials. Bioresour. Technol. 95(3), 343-350.

[15] Suni, S., Kosunen, A.L., Hautala, M., Pasila, A., Romantschuk, M., 2004. Use of a by-product of peat excavation, cotton grass fibre, as a sorbent for oil-spills. Mar. Pollut. Bull. 49(11-12), 916-921.

[16] Viraraghavan, T., Mathavan, G.N., 1988. Treatment of oil-in-water emulsions using peat. Oil and Chemical Pollution 4(4), 261-280.

[17] Banerjee, S.S., Joshi, M.V., Jayaram, R.V., 2006. Treatment of oil spill by sorption technique using fatty acid grafted straw. Chemosphere 64(6), 1026-1031.

[18] Inagaki, M., Kawahara, A., Konno, H., 2002. Sorption and recovery of heavy oils using carbonized fir fibers and recycling. Carbon 40(1), 105-111.

[19] Ibrahim, S., Ang, H.M., Wang, S., 2009. Removal of emulsified food and mineral oils from wastewater using surfactant modified barley straw. Bioresour. Technol. 100, 5744–5749.

[20] Ibrahim, S., Wang, S., Ang, H.M., 2010. Removal of emulsified oil from oily wastewater using agricultural waste barley straw. Biochem. Eng. J. 49, 78–83.

[21] Husseien, M., Amer, A.A., El-Maghraby, A., Taha, N.A., 2009. Availability of barley straw application on oil spill cleanup. Int. J. Environ. Sci. Te. 6 (1), 123–130.

[22] Hussein, M., Amer, A.A., Sawsan, I.I., 2008a. Oil spill sorption using carbonized pith bagasse: 1. Preparation and characterization of carbonized pith bagasse. J. Anal. Appl. Pyrol. 82(2), 205-211.

[23] Sun, R.C., Sun, X.F., Sun, J.X., Zhu, Q.K., 2004b. Effect of tertiary amine catalysts on the acetylation of wheat straw for the production of oil sorption-active materials. C. R. Chim. 7, 125–134.

[24] Sun, X.F., Sun, R.C., Sun, J.X., 2002. Acetylation of rice straw with or without catalysts and its characterization as a natural sorbent in oil spill cleanup. J. Agric. Food Chem. 50 (22), 6428–6433.

[25] Kumagai, S., Noguchi, Y., Kurimoto, Y., Takeda, K., 2007. Oil adsorbent produced by the carbonization of rice husks. Waste Manage. 27 (4), 554-561.

[26] Angelova, D., Uzunov, I., Uzunova, S., Gigova, A., Minchev, L., 2011. Kinetics of oil and oil products adsorption by carbonized rice husks. Chem. Eng. J. 172, 306– 311.

[27] Sayed, S.A., Zayed, A.M., 2006. Investigation of the effectiveness of some adsorbent materials in oil spill clean-ups. Desalination 194 (1-3), 90-100.

[28] Sathasivam, K., Haris, M.R.H.M., 2010. Adsorption kinetics and capacity of fatty acidmodified banana trunk fibers for oil in water. Water Air Soil Pollution 213, 413–423.

[29] Nwokoma, D.B., Anene, U., 2010. Adsorption of crude oil using meshed groundnut husk. Chemical Product and Process Modeling 5 (1, 9), 1–21.

[30] Batzias F. A., Sidiras D.K., Siontorou C.G., Bountri

A.N., Politi D.V.. Fuzzy Multicriteria Ranking Of Waste Materials To Be Used As Adsorbents Within An Industrial Ecology Framework. 10th WSEAS International Conference on ENVIRONMENT, ECOSYSTEMS and DEVELOPMENT (EED '12), Advances in Environment, Computational Chemistry and Bioscience, Montreux, Switzerland, December 29-31, 2012. pp. 236-241.

[31] Sidiras D.K., Batzias F. A., Siontorou C.G., Bountri A.N., Politi D.V. Simulation Of Biomass Thermochemical Modification And Hydrocarbons Adsorption/Desorption. 21st European Biomass Conference and Exhibition. Copenhagen, Denmark, 3 - 7 June 2013, pp. 1035-1049.

[32] Sidiras D., Batzias F., Konstantinou I., Tsapatsis M. Simulation of autohydrolysis effect on adsorptivity of wheat straw in the case of oil spill cleaning. Chemical Engineering Research and Design, In Press, Corrected Proof, Available online 21 December 2013, http://dx.doi.org/10.1016/j.cherd.2013.12.013.

[33] Katsamas G., Sidiras D.. Sugars Production from Wheat Straw Using Maleic Acid. RECENT ADVANCES in CHEMICAL ENGINEERING, BIOCHEMISTRY and COMPUTATIONAL CHEMISTRY. In Proc. 4th European Conference of Chemical Engineering (ECCE '13) Paris, France, October 29-31, 2013, pp. 23-28.

[34] DIN 66132, Determination of specific surface area of solids by adsorption of nitrogen; single-point differential method according to Haul and Dümbgen (1975).

[35] Saeman, J.F., Bubl, J.F., Harris, E.E, 1945, Quantitative saccharification of wood and cellulose. Ind. Eng. Chem. Anal. Ed., 17, 35-7.

[36] Somogyi M. Notes on Sugar Determination. J. Biol. Chem. 1952; 195: 19.

[37] Tappi Standards, Tappi Tests Methods, T222 om-88, Atlanta (1997).

[38] American Society of Testing and Materials - International, ASTM F 726-06, Standard Test Method for Sorbent Performance of Adsorbents, West Conshohocken (2006) 1201-1206.

[39] Abatzoglou N., Chornet E., Belkacemi K., 1992. Phenomenological kinetics of complex systems: the development of a generalized severity parameter and its application to lignocelulosics fractionation, Chem. Eng. Sci., 47(5), 1109-1122.

[40] Garrote, G., Cruz, J.M., Domínguez, H., Parajó, J.C., 2008. Non-isothermal autohydrolysis of barley husks: Product distribution and antioxidant activity of ethyl acetate soluble fractions, J. Food Eng. 84(4), 544-552.

[41] Kabel, M.A., Bos, G., Zeevalking, J., Voragen, A.G.J., Schols, H.A., 2007. Effect of pretreatment severity on xylan solubility and enzymatic breakdown of the remaining cellulose from wheat straw. Bioresour. Technol. 98, 2034–2042

[42] Lee, J.W., Jeffries T.W., 2011. Efficiencies of acid catalysts in the hydrolysis of lignocellulosic biomass over a range of combined severity factors. Bioresour. Technol. 102, 5884–5890.

[43] Freundlich HMF (1906) Über die adsorption in lösungen, Zeitschrift für Physikalische Chemie. 57:385-471.

[44] Langmuir I (1916) The constitution and fundamental properties of solids and liquids. J Am Chem Soc 38:2221-2295.

[45] Sips R, 1948, Structure of a catalyst surface. J Chem Phys 16:490-495.

[46] Radke CJ, Prausnitz JM, 1972, Adsorption of Organic Solutes from Dilute Aqueous Solution on Activated Carbon. Ind Eng Chem Fundam 11:445-451.

[47] Weber WJ , Morris JC, 1963, Kinetics of adsorption on carbon from solution. J Sanit Eng Div Am Soc Civ Eng 89 :31-60.

[48] Toth J, 2000, Calculation of the BET-compatible surface area from any Type I isotherms measured above the critical temperature. J Colloid Interface Sci 225:378-383.

[49] Temkin MJ, Pyzhev V, 1940, Recent modification to Langmuir isotherms, Acta Physiochim, URSS 12:217–222.

[50] Dubinin M, Radushkevich L, 1947, Equation of the characteristic curve of activated charcoal. Chem. Zentr 1:875-890.

[51] Lagergren S (1898) Zur theorie der sogenannten adsorption gelöster stoffe. Kungliga Svenska Vetenskapsakademiens, Handlingar 24:1-39.

[52] Ho YS, Ng JCY, McKay G, 2000, Kinetics of pollutants sorption by biosorbents: review. Sep Purif Methods 29:189-232.

[53] Batzias F.A., Konstantinou I.G., Vallaj N.L., Sidiras D.K, Diminishing an oil-products spill in seawater by using modified lignocellulosic residues as low cost adsorbents. Proc. 19th International Congress of Chemical and Process Engineering CHISA 2010. Prague, Czech Republic, 28 August - 1 September 2010, No 1388.

6 ACKNOWLEDGEMENTS

7 LOGO SPACE